RESEARCH PAPER

3D Coupled Thermal-Electrical-Structural Finite Element Investigation on the Effect of Welding Parameters on the Geometry of Nugget Zone and HAZ in RSWed TRIP Steel joints

Ali Ebrahimpour[1],*, Amir Mostafapour[2], Naeimeh Haghi[2]

* aliebrahimpour414@gmail.com

[1] Mianeh Technical and Engineering Faculty, University of Tabriz, Tabriz, Iran
[2] Mechanical Faculty, University of Tabriz, Tabriz, Iran

Abstract: In this research, the effect of resistance spot welding (RSW) parameters including current intensity, welding time and welding force (coded by A, B and C) on the radius, thickness and area of the nugget and the radius of the heat affected zone(HAZ) of transformed induced plasticity (TRIP) steel joints was investigated by design of experiment(DOE) and response surface methology (RSM). A 3D coupled thermal-electrical-structural FEM was used to model RSW. To validate the FE model, two TRIP steel sheets were welded experimentally. During welding, the temperature was measured and the results were compared with the FE results and a good agreement was obtained. The boundaries of the welding zones were determined according to the critical temperatures and the responses in all samples were calculated. Using analysis of variance, direct, quadratic and interaction effects of parameters on the responses were studied and a mathematical model was obtained for each response. The direct linear effect of all parameters on all responses were significant. But among the interaction effects, the effect of B×C on the nugget radius, the effect of A×B on the nugget thickness, the effect of A×B on the nugget area and the effects of A×B and B×C on the HAZ radius were significant. Also, current intensity had the greatest effect on all responses.

Keywords: RSW, TRIP steel, Finite element modeling, Response surface methodology, Nugget, HAZ.

1. INTRODUCTION

The use of advanced high strength steels (AHSS) in various industries, especially in the automotive industry, due to high strength and reducing the final weight of the car and reducing fuel consumption, is facing a significant increase. The AHSS steels can be summarized as: dual phase (DP) steels, transformed induced plasticity (TRIP) steels, complex phase (CP) steels and martensitic (M) steels [1]. Among AHSS steels, TRIP steels are very important due to their excellent combination of strength and ductility. These steels have various phases in their microstructure, including ferrite, bainite, retained austenite, and possibly partially martensite [2].

In the microstructure of TRIP steel, retained austenite is transformed to martensite during deformation, which increases the strength and ductility of the material [1]. One of the limitations for the widespread use of TRIP steel is the weldability [3].

TRIP steel is most commonly used in sheet form in industries such as automotive industry and spot joint is usually used to connect the sheets in the car body. One of the most common methods for

spot welding is resistance spot welding (RSW), which is widely used in automotive, aerospace, railway, etc. industries [4]. RSW is especially important in the automotive industry, where 90% of car body assembly is done by this method [5]. One of the main advantages of RSW is the ability to automate. However, in RSW metal undergoes in the interaction effect of various phenomena such as: electrical, mechanical, thermal, fluid flow and metallurgical phenomena. This interaction effects of various phenomena makes the nature of RSW complicated and as a result, it faces many problems in controlling [6]. During the RSW process, two metal sheets are pressed together by the electrode force and then due to the passage of electric current and resistance between the two sheets (which is greater than the resistance of the sheets and the resistance between the sheets and electrodes at the beginning of the process [7]) thermal energy is created between them. The welding time is very short and the force of the electrodes is still applied during the passage of current. The amount of energy produced between the two sheets is calculated through the following equation:

$$Q = \int_{t_1}^{t_2} I^2(t)\, R(t)\, dt, \tag{1}$$

where Q is generated heat during welding in Joule, t_1 and t_2 respectively are the starting and finishing time of the current passing, I(t) is the current intensity, R(t) is the total resistance between two electrodes [8]. The heat generated increases the temperature of the contact area between the two sheets and causes part of the metal to melt. The higher the heat, the more metal melts and form the liquid nugget. According to Equation 1, the amount of generated heat depends on the current intensity, electrical resistance, and welding time. The electrical resistance R (t) is a variable parameter and is called the dynamic resistance, which can almost indicate the resistance of the welding load, because the effects of other parameters are generally ignored. When the amount of molten metal reaches a certain level, the delivery of external electrical energy ends, then the molten metal solidifies and the metal parts are joined together. [4].

Although tensile-shear strength has traditionally been measured for joint quality in RSW, obtaining this strength requires a costly, time-consuming and destructive test. However, some researchers have measured the strength of welding joints to assess quality [9-13]. In the meantime, some of researchers have studied the tensile-shear strength of RSWed TRIP steel joints [14-16]. An alternative method to check the quality of the RSW joint is to investigate the geometry of the nugget zone (NZ) and heat affected zone (HAZ). In some previous studies, the effect of parameters on the weld zone geometries has been studied experimentally. In one of these works, Dickinson et al. [7] studied the relationship between RSW input parameters and weld phenomena considering their effects on dynamic resistance. In another study, Akash et al. [17] investigated the effect of welding current and welding time on NZ size in RSW of steel. In this study, the current intensity was in the range of 6 to 11.5 kN and the welding time was in the range of 5 to 30 cycles. The NZ size was measured using an optical microscope and the results were supported by diagrams. Finally, appropriate welding parameters were advised to the users. Wen et al. [18] investigated the effect of current intensity, welding time and welding force on the diameter of the NZ in RSW of steel. They reported that the nugget diameter increases with increasing current intensity but decreases as it continues. Also, according to the results presented in their study,

the nugget diameter increases with increasing welding time as result of increasing the generated heat.

Conducting experimental studies to investigate the effect of RSW parameters on the size of NZ and HAZ cannot provide comprehensive information over a wider range of parameters due to cost, time and difficulty constraints. Therefore, many researchers have used numerical and finite element methods (FEM) to achieve this goal [5, 6, 14, 19-21]. Eissazadeh et al. [19] simulated RSW of 1008 steel using FEM and investigated the effect of welding parameters on the formation of the nugget and its thickness. They reported that increasing the current intensity increases the nugget thickness. In a technical report, Eshraghi et al. [20] investigated the effect of welding parameters on the geometry of welding areas using the FEM in RSW of DP steels. The results published in this report indicate that the current intensity has the greatest influence on the geometry of the weld zone. Zhang et al. [21] investigated the effect of electrode force on expulsion phenomenon and nugget size in RSW of DP steel sheets that have an initial gap before joining, using FEM. They report that increasing the force of the electrode can prevent an explosion and reduce the radius of the nugget.

As mentioned, RSW is a complex process that is affected by various parameters and therefore the geometry of the NZ and HAZ is also a function of various parameters such as current intensity, welding time, welding force, geometry and material of the electrode, sheet thickness and cooling conditions. Numerous studies have reported that the first three parameters (current intensity, welding time and welding force) are the most important factors influencing the welding zones [4]. Careful examination of the effect of different parameters on a response requires numerous experiments. Therefore, the use of a suitable design of experiments (DOE) to reduce the number of runs while reducing the probability of error has been considered by many studies. Response surface methodology (RSM) has been used as a DOE method in some RSW related researches and has yielded good results [20].

By reviewing previous studies, it can be concluded that a detailed and comprehensive study of the effect of welding parameters on the size of NZ and HAZ in the RSW of TRIP steel sheets has not been done so far. Therefore, in this study, the

2

effect of current intensity, welding time and welding force on the radius, thickness and area of the NZ and the radius of the HAZ was performed using coupled thermal-electrical-structural finite element simulation. For this purpose, a DOE by RSM was used and the direct and quadratic effect of each parameter and their interaction effect on the responses were investigated using analysis of variance (ANOVA).

2. EXPERIMENTAL PROCEDURES

2.1. Finite element Model

A 3D coupled thermal-mechanical-electrical modeling was used to simulate the RSW process. Abaqus 2019 software was used for this purpose. Simulation of the RSW process is very complex due to the interaction of electrical, thermal, metallurgical and mechanical phenomena. Fig. 1 shows a schematic model of the interaction of various phenomena in the RSW process. Two methods are typically used for modeling of RSW.

The first method is weak coupling in which first a thermal-electrical analysis is performed and then a mechanical analysis is performed considering the outputs of the previous analysis. But in the second method, which is called strong coupling, thermal-electrical and mechanical analyzes are performed simultaneously. Abacus can do both methods, but we used a strong coupling because it models the real welding conditions more accurately [20].

The model geometry consists of two TRIP steel sheets with dimensions of $30 \times 100 \times 1.2$ mm and two copper alloy electrodes with tip radius of 3 mm, which are shown in Fig. 2. Due to symmetry and to reduce the solving time, only a quarter of the geometry of the parts was modeled. Some temperature-dependent properties of sheets given to the software are shown in Fig. 3 [3]. The Poisson's ratio was considered to be 0.3. the thermal and electrical contact conductance of sheet/sheet and electrode/sheet and electrical conductivity obtained from reference [20].

Fig. 1. Schematic diagram showing the interaction between various phenomena in the RSW process.
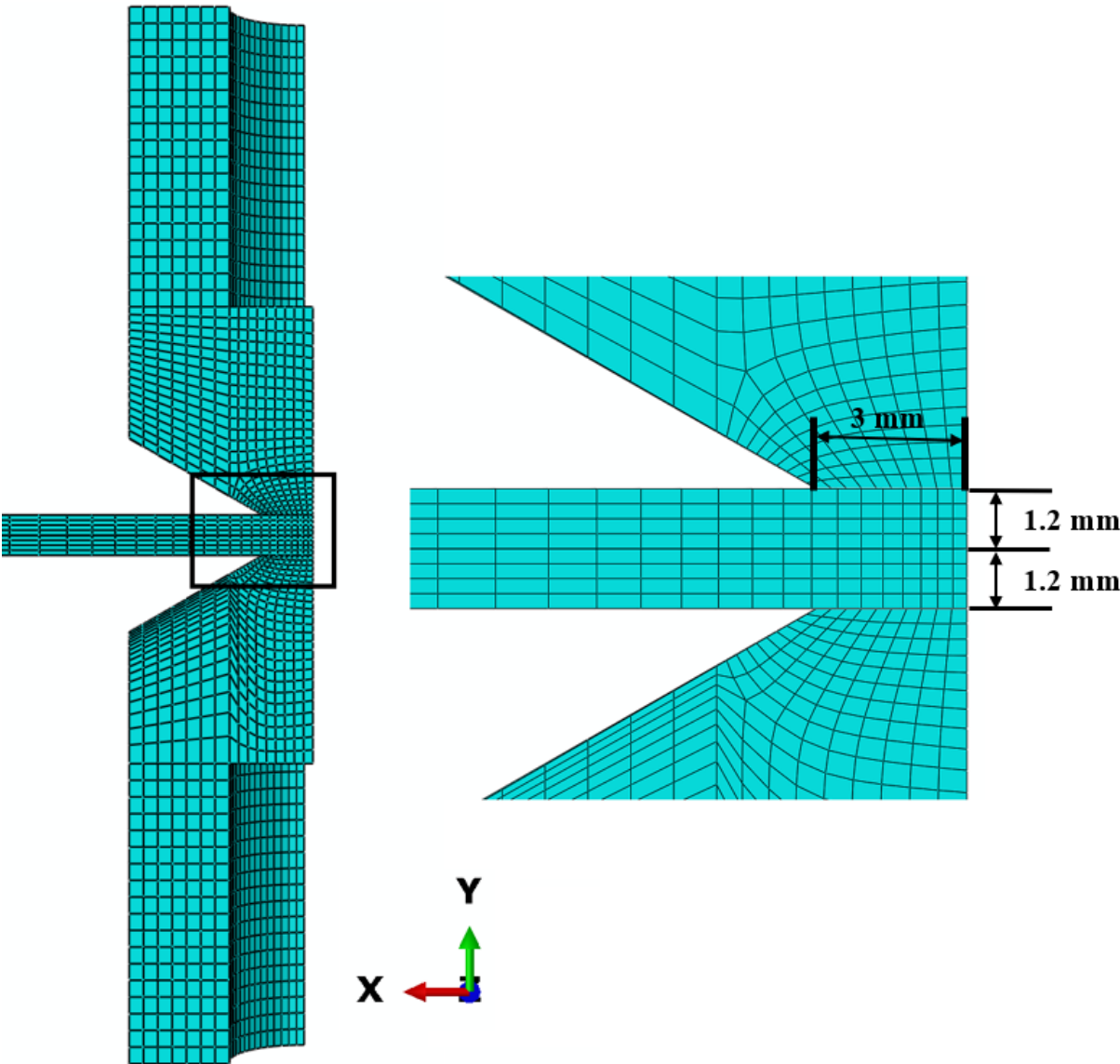
Fig. 2. The finite element model geometry and mesh.

Fig. 3. Temperature dependent (a) mechanical properties and (b) physical properties of TRIP steel.

An 8-node brick, trilinear displacement, electric potential and temperature element (which coded by Q3D8 in Abaqus) were used for meshing the workpieces. As shown in Fig. 2, the size of the elements near the contact area is smaller to increase the accuracy of the results for temperature and other outputs. Mesh analysis was used to obtain the appropriate element size. For this purpose, by performing several runs and comparing the obtained temperatures, the size of

4

the smallest element was selected equal to 0.3 mm and the total number of sheet elements was 24,000. The lower surface of the lower electrode is bounded in the Y direction. All surfaces except the contact surfaces with the electrodes and the contact surface of the two sheets have convective heat transfer. The voltage at the lower electrode is zero. The initial temperature of the workpiece is 25°C. The main purpose of this study is to investigate the effect of three welding parameters: current intensity, welding time and welding force on the size of the NZ and HAZ. To determine the boundaries of the NZ and HAZ, it is necessary to know the liquidous, solidus, Ac_1 and Ac_3 temperatures. These temperatures were calculated by Termo-Calc software and the values of 1530°C, 1480°C, 836°C and 705°C were obtained. The total time in RSW process is divided into 4 parts: (1) the time of applying the compressive force of the electrodes on the sheets, (2) The time of passage of AC electric current at the same time as the compressive force of the electrodes continues (this time is called welding time), (3) Time to continue the compressive force of the electrodes after stopping the electric current (forging time) and finally (4) the cooling time. The parameter of welding time is the second stage, ie the passage time of electric current. Since the frequency of electric current in all samples is equal to 60 Hz, the welding time in this study is presented as the number of cycles.

2.2. Finite Element Model Validation

In order to validate the FE model and also the microstructural studies of the welding areas, by performing an experimental test, two TRIP steel sheets with dimensions equal to the dimensions of the FE model and the same input parameters were welded. In this experimental test, welding parameters were set to 8 kA, 20 cycles and 3 kN for current intensity, welding time and welding forces. For this purpose, a steel with chemical composition 0.21 C, 1.5 Si, 1.68 Mn, 0.03 Cr, 0.016 Al, 0.01 Ni and 0.009 S (wt.%) was produced by casting and then hot rolled. Then, a steel sheet with a thickness of 1.2 mm was obtained by cold rolling. A two-stage heat treatment was used to obtain the multiphase microstructure of trip steel. The first stage is called intercritical annealing (IA), which the volume fraction of austenite and ferrite is controlled in temperature between Ac_1 and Ac_3.

The second stage is performed immediately after IA, in which the steel is kept isothermally in the temperature range of the bainite transformation, which is called the isothermal bainite transformation (IBT). At this stage, part of the austenite is transformed to bainite and causes the stability of the retained austenite [22, 23]. To produce TRIP steel, temperatures of 790°C and 350°C were used for stages IA and IBT, respectively [14]. Field emission scanning electron microscope (FE-SEM) and optical microscopy (OM) were used to study the micro and macrostructure and X-ray diffraction (XRD) method was used to measure the percentage of retained austenite. Also, the microhardness of the samples was measured by Vickers method under the force of 100 g. The sample temperature during welding was obtained by connecting a K type thermocouple to the bottom surface of the lower sheet.

2.3. Design of Experiments

After validating the FE model, a three-factor Box-Behnken design of RSM was used to find the relationship between input parameters and responses. In this study the input parameters are, current intensity, welding time and welding force which are coded as A, B and C, respectively. Given that each parameter has three levels (-1, 0 and 1), the number of experiments with full factorial design will be 27 runs. By using a Box-Behnken fractional factorial design, the number of experiments was reduced to 15 runs, which can still predict the relationship between parameters and responses well. Also, the responses are, NZ radius, NZ thickness, NZ area and HAZ radius.

Analysis of variance (ANOVA) technique was employed using Minitab software to describe the output. The main and interaction effects of parameters are considered in ANOVA and the significance of their effects on response is investigated (for significance the *p-value* of model or its terms must be less than 0.05).

For correlation of input variables and the response, a mathematical model with the ability to predict the linear, quadratic, and interaction effects of the parameters on the responses was designed according to experiments outputs. Using RSM, a second-order polynomial mathematical model to predict the main, quadratic, and interaction effects of inputs on output, can be obtained. In this equation the response can

be given according to the values of the parameters [3]:

$$y = \beta_0 + \sum_{j=1}^{k} \beta_j x_j + \sum_{j=1}^{k} \beta_{jj} x_j^2 + \sum_{i<j} \sum_{j=2}^{k} \beta_{ij} x_i x_j \qquad (2)$$

Where β_0 is a constant and β_{ij} is called the regression coefficient. Also, *x* refers to any of the parameters. According to the data published in the previous studies, the RSW parameters must be within an acceptable range which is called welding lobe [24] to ensure the final quality of the weld is appropriate. In the present study, the range of parameters was selected considering previous experimental studies of AHSS steels [15, 20, 25]. This makes it possible to compare the results of finite element modeling in this research with the results obtained in previous experimental and finite element research. The values, ranges and levels of parameters are presented in Table 1.

3. RESULTS AND DISCUSSION

3.1. Experimental Results and FE Model Validation

Fig. 4 shows the section views of experimentally RSWed sample and FE output of case number 13. In the experimental sample, NZ and HAZ and base metal (BM) are recognizable according to their macro appearance. In the FE model, these zones are marked according to the temperature distribution. There is a very good match between the size of these areas.

Table 1. Real and coded values of parameters and calculated values of responses.

Run number	A	B	C	Current (kA)	Time (cycles)	Force (kN)	Nugget Radius (mm)	Nugget Thickness (mm)	Nugget Area (mm^2)	HAZ Radius (mm)
1	-1	-1	0	6	10	3	0.7	0.10	0.22	2.4
2	1	-1	0	10	10	3	2.5	0.61	4.71	3.1
3	-1	1	0	6	30	3	1.5	0.20	0.94	2.48
4	1	1	0	10	30	3	3.41	1.45	15.53	3.87
5	-1	0	-1	6	20	2	2.07	0.31	1.95	2.78
6	1	0	-1	10	20	2	3.2	0.97	9.75	3.8
7	-1	0	1	6	20	4	1.2	0.1	0.37	2.52
8	1	0	1	10	20	4	3.01	0.59	5.56	3.3
9	0	-1	-1	8	10	2	2.1	0.58	3.82	2.84
10	0	1	-1	8	30	2	3.2	1.2	12.06	3.78
11	0	-1	1	8	10	4	1.8	0.14	0.79	2.54
12	0	1	1	8	30	4	1.89	0.54	3.20	2.58
13	0	0	0	8	20	3	3.1	1.01	9.83	3.92
14	0	0	0	8	20	3	3.1	1.02	9.93	3.91
15	0	0	0	8	20	3	3.1	1.02	9.93	3.92

Fig. 4. Comparison of weld zone cross section in experimental sample and finite element model (welding parameters were set to 8 kA, 20 cycles and 3 kN for current intensity, welding time and welding forces)

Fig. 5 compares the finite element and experimental thermal history of a point on the bottom surface of the lower sheet. Despite the slight difference, the simulation results are in acceptable agreement with the experimental results. This small difference is due to the complexity of the welding process, which has been reported in most studies and its validity has been confirmed [26]. On the other hand, the maximum temperature obtained in the finite element model is about 2500°C. This value is very close to the reported temperatures for AHSS steels RSWed under similar conditions [21].

Fig. 5. Comparison of the thermal history of a point at the lower lower surface of the lower sheet in the experimental sample and the finite element model (welding parameters were set to 8 kA, 20 cycles and 3 kN for current intensity, welding time and welding forces).

Fig. 6 shows the microstructure of BM, HAZ, and NZ. In the BM, ferrite is seen in a completely dark color as the field phase. The bainite phase is clearly visible with a layered structure consisting of bainitic ferrite and retained austenite (A/B in Fig. 6(a)). The retained austenite is seen as uncut grains with a perfectly smooth and clear surface. Unlike austenite, martensite has a rough surface that makes it easier to identify; Detection of martensite from austenite is possible only through the smoothness and roughness of the surface of these two phases. Detection of these phases in the same type of TRIP steel has been reported in previous studies [2, 3, 23, 27]. The percentage of retained austenite in the microstructure of BM and welding zones are measured by XRD and are given in Fig. 7. Fig. 7 also shows the microhardness along the horizontal line passing through the center of the cross section. According to this figure, the percentages of retained austenite and microhardness of BM are equal to 12% and 250 VHN, respectively. According to the maximum temperature, the HAZ can be divided into at least two subdivided zones. In parts where the temperature rises to between Ac_1 and Ac_3, part of the ferrite is transformed to austenite. On the other hand, in parts where the temperature exceeds Ac_3, the whole microstructure is transformed to austenite. When austenite cools, it can be converted to ferrite, bainite and martensite due to the cooling rate. Fig. 6(b) shows the microstructure of HAZ where the temperature has risen to a temperature between Ac_1 and Ac_3. The main phases are ferrite and martensite, but a small amount of retained austenite is also detectable. A decrease in the percentage of retained austenite to 7% and an increase in the microhardness to about 370 VHN as shown in Fig. 7 confirm this observation.
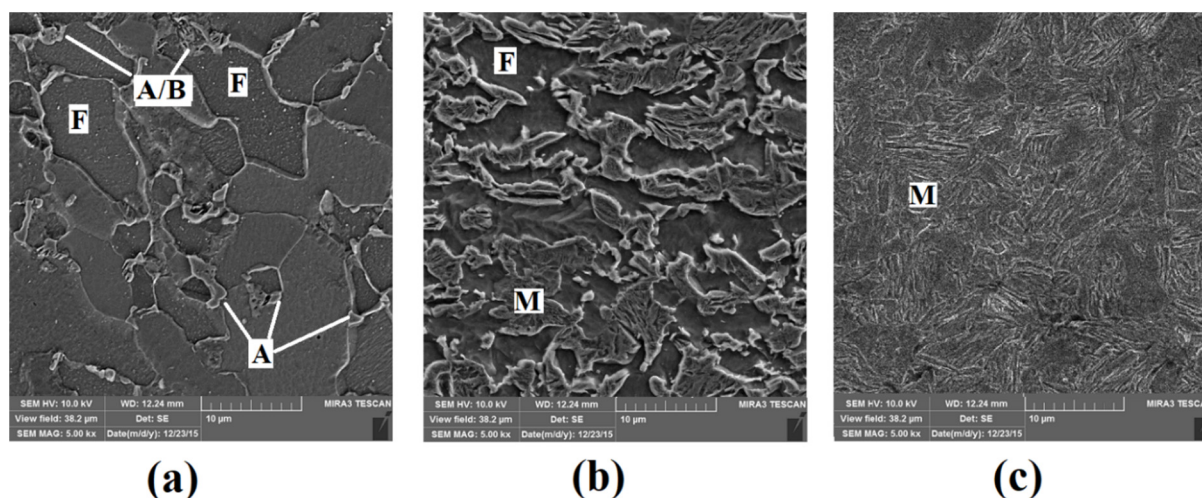

Fig. 6. FE-SEM microstructure of (a) BM, (b) HAZ, and (c) NZ in experimentally welded sample.

Ali Ebrahimpour, Amir Mostafapour, Naeimeh Haghi

In the NZ, the temperature is higher than the melting point and the material melts. During cooling, austenite is formed first and due to the cooling rate, which is very high, all the microstructure transforms to the martensite. As can be seen from Fig. 7, the percentage of retained austenite in this zone is zero and the microhardness has reached 498 VHN with a sharp increase. The all-martensitic microstructure of this area can also be seen in Fig. 6(c).

Fig. 7. Microhardness and retained austenite percentage in welding zone.

3.2. ANOVA Results

Fig. 8 shows temperature distribution in all cases. Based on the critical temperatures, NZ and HAZ are distinguished by different colors. Based on the change in the values of parameters in each case, the heat distribution changes and as a result, the size of the areas is different. NZ and HAZ sizes were measured in each of the cases and the results are presented in Table 1.

It should be noted that in samples 4 and 10, due to excessive increase in input heat, the thickness of the nugget continues to the outer surface of the sheets, and also due to thermal expansion, this thickness exceeds the total thickness of the sheets. This reduces the quality of the weld and leads to the distance of the sheets from each other and eventually leads to expulsion. These defects have also been reported in previous studies [20].

In factorial DOE, ANOVA is used to determine the significance of model and model terms. A model or model term is significant when its *p*-value is less than 0.05.

The ANOVA for the responses as influenced by the input variables is shown in Tables 2. As can be seen from this table, the direct linear and quadratic effects of all three parameters (A, B and

C) on the all responses are significant except the quadratic effect of B (B×B) on the nugget thickness. Regarding the interaction effects of the parameters, the effect of B×C on the nugget radius, the effect of A×B on the nugget thickness, the effect of A×B on the nugget area and the effects of A×B and B×C on the HAZ radius are significant.

For prediction of responses within the design space, the mathematical models are given in terms of coded factors as:

Nugget radius (mm)= 3.1000 + 0.8300 A + 0.3625 B - 0.3350 C - 0.4763 A×A - 0.5963 B×B- 0.2562 C×C + 0.0275 A×B + 0.1675 A×C - 0.2525 B×C   (3)

Nugget thickness (mm)= 1.0167 + 0.3637 A + 0.2463 B - 0.2100 C - 0.2771 A×A - 0.1521 B×B- 0.2496 C×C + 0.1875 A×B - 0.0450 A×C - 0.0550 B×C   (4)

Nugget area (mm²)= 9.901 + 4.008 A + 2.774 B - 2.207 C - 2.556 A×A -1.994 B×B - 2.936 C×C+ 2.525 A×B - 0.654 A×C - 1.456 B×C   (5)

HAZ radius (mm)= 3.9167+ 0.4862 A+ 0.2288 B- 0.2825 C- 0.3946 A×A- 0.5596 B×B-0.4221 C×C+ 0.1725 A×B-0.0600 A×C-0.2250 B×C   (6)

3.3. Model Validation

To confirm the validity of the proposed model, three confirmation welding simulations were performed in which the parameters were randomly changed in the range of model values. The actual results, which were the average of the three modeling results for each response, are shown in Table 3, along with the predicted values and the error percentage calculated in the experiments.

The low percentage of error between the actual and predicted values for the answer indicates that the proposed model can predict the results with a good approximation.

3.4. Parameters Effect

As can be seen from Table 2, the direct linear and quadratic effects of all three parameters on the nugget radius are significant. But only the interaction effect of welding time and welding force is significant and the current intensity with the other two parameters does not cause a significant interaction effect.

Fig. 9(a) represents the direct effect of welding parameters on the nugget radius. Increasing the welding current from 6 kA to 10 kA creates nuggets with a larger radius.

Fig. 8. Finite element outputs for all cases (the welding parameters values in each case are listed in Table 1)

Although the increasing rate nugget radius is much higher in lower current intensity, but as we approach 10 kA current, this rate decreases and a tendency to stop the larger nugget radius is observed. Similar results have been reported in previous research [14, 17, 18, 20, 28-30]. Akash *et al*. [17] investigated the effect of current intensity and welding time on the nugget size in RSW of two steel sheets at constant welding force. In this study, the current intensity ranged from 6 kA to 11.5 kA and the welding time ranged from 10 to 30 cycles. They report that with increasing current intensity, the nugget radius increases, but at currents above 10 kA, the

9

increase in nugget radius stops due to excessive heat rise and return of the electrodes due to thermal expansion. Wan et al. [30] established a model to explore the effect of welding current on RSW of DP steel sheets. They predicted the nugget size by FEM and by varying the current intensity in the range of 6 kA to 12 kA. The final results showed that the nugget size and shape were highly dependent on the welding current. Also, the expulsion phenomenon was also considered in the work. It occurred at 12 kA and unsatisfactory partial interfacial failure can be detected.
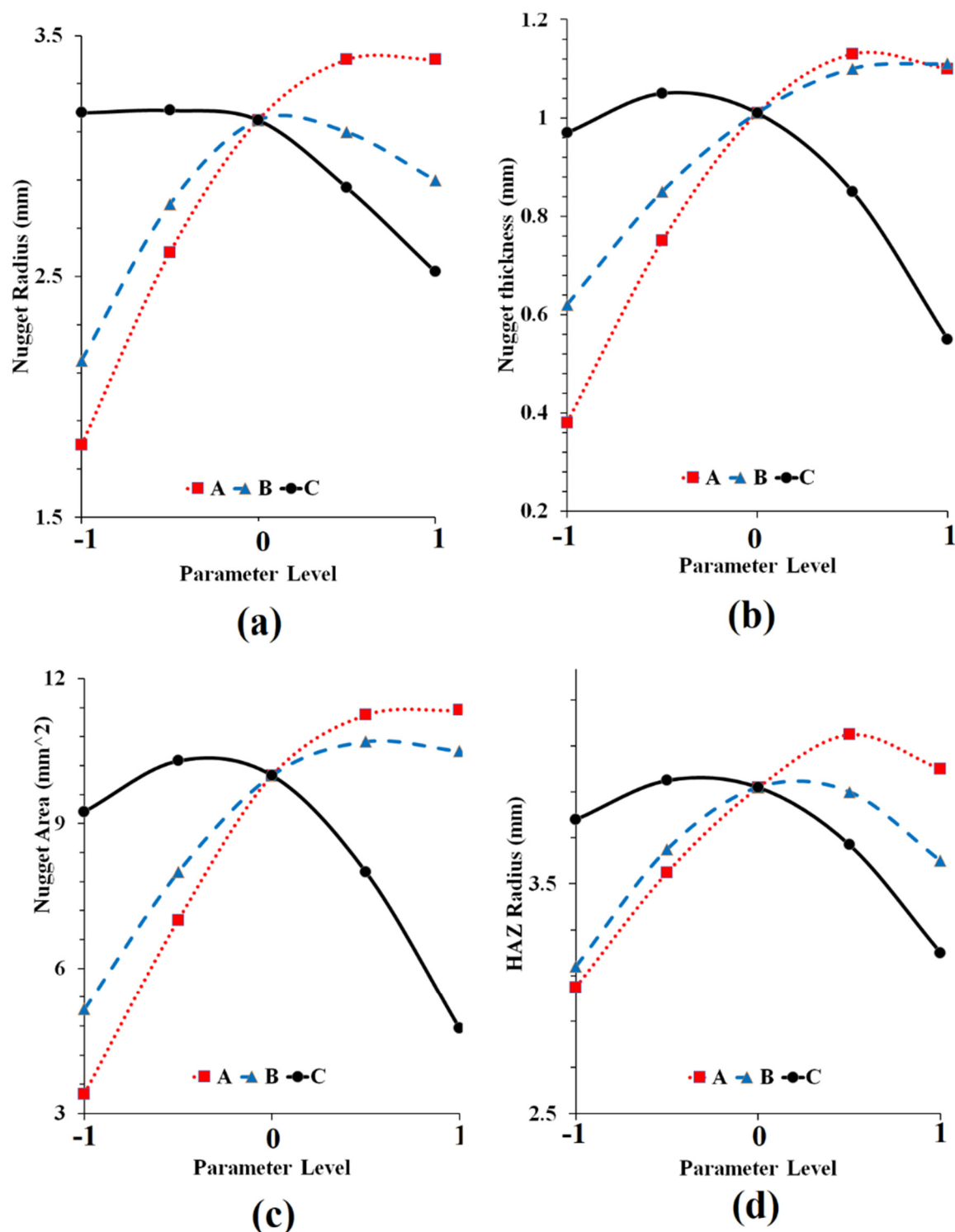

Fig. 9. Mean effect of parameters on (a) NZ radius, (b) NZ thickness, (c) NZ area, and (d) HAZ radius.

10

Table 2. ANOVA results for all responses.

Source	Nugget Radius		Nugget Thickness		Nugget Area		HAZ Radius	
	F-Value	P-Value	F-Value	P-Value	F-Value	P-Value	F-Value	P-Value
Model	37.79	0	18.4	0.003	19.19	0.002	36.75	0
Linear	84.99	0	40.53	0.001	40.41	0.001	60.56	0
A	188.35	0	67.86	0	68.02	0	116.56	0
B	35.93	0.002	31.1	0.003	32.59	0.002	25.8	0.004
C	30.68	0.003	22.62	0.005	20.62	0.006	39.34	0.002
Square	24.16	0.002	11.24	0.012	10.86	0.013	42.78	0.001
A*A	28.62	0.003	18.17	0.008	12.76	0.016	35.42	0.002
B*B	44.86	0.001	5.47	0.066	7.76	0.039	71.24	0
C*C	8.29	0.035	14.75	0.012	16.84	0.009	40.53	0.001
2-Way Interaction	4.22	0.078	3.44	0.109	6.29	0.038	6.9	0.032
A*B	0.1	0.761	9.02	0.03	13.49	0.014	7.33	0.042
A*C	3.84	0.108	0.52	0.503	0.91	0.385	0.89	0.389
B*C	8.72	0.032	0.78	0.419	4.48	0.088	12.48	0.017
Lack-of-Fit	0.001	790.5	779.25	0.001	995.59	0.001	810.75	0.001
	R-sq	R-sq (adj)	R-sq	R-sq (adj)	R-sq	R-sq (adj)	R-sq	R-sq (adj)
	98.55%	95.94%	97.07%	91.79%	97.19%	92.12%	98.51%	95.83%

Table 3. The results of validation for all mathematical models.

A	B	C	Nugget radius (mm)			Nugget thickness (mm)		
			predicted	actual	error	predicted	actual	error
-0.7	0.5	-0.5	2.533388	2.64	4.3%	0.686354	0.7	2.9%
0.25	-0.25	0.5	2.969063	2.82	4.9%	0.841354	0.89	5.9%
0.75	0.25	0.25	3.428984	3.52	2.9%	1.140859	1.08	5.7%
A	B	C	Nugget area (mm^2)			HAZ radius (mm)		
			predicted	actual	error	predicted	actual	error
-0.7	0.5	-0.5	6.35268	5.8	8.60%	3.368029	3.23	3.80%
0.25	-0.25	0.5	8.030109	7.88	1.80%	3.684479	3.81	3.60%
0.75	0.25	0.25	11.56323	1.94	3.20%	3.991641	4.16	4.40%

In fact, when welding current exceeded 10 kA, excessive welding current induced a weld expulsion and the nugget diameter decreased accordingly [18]. Expulsion is a negative phenomenon which can seriously affect the weld quality during the welding process and a lot of previous works concerned it [4]. Expulsion occurs when the radius of the nugget is greater than the radius of the contact area of the two sheets [21]. According to the *F*-value (in Table 1), which indicates the effect of a parameter on the response, it can be seen that the current intensity has the highest *F*-value and therefore has the greatest effect on the nugget radius that can be explained by the generated heat equation (Equation 1).

Increasing the welding time from 10 to 20 cycles increases the nugget radius and further increasing the welding time from 20 to 30 cycles reduces the radius. In fact, the growth of the nugget radius continues until the expulsion occurs [26]. In samples 4, 6, 10 and 13, where the current intensity and welding time are high, the growth of the radius has stopped due to the occurrence of the expulsion phenomenon. These results have been confirmed in previous reports [17]. Dynamic resistance and electrode displacement have been reported to be two important signals for the weld quality. These two signals can provide useful information about what is happening inside the welding zone. Fig. 10 shows the typical dynamic resistance and electrode displacement behavior during RSW of carbon steels [31]. At the beginning, the amount of dynamic resistance is high, which decreases very quickly as soon as force squeezes the sheets. Then, with heat generation, the temperature and the dynamic resistance increase. But as the temperature

continues to rise, the metal melts and liquid nugget forms. By applying force, the distance between the two electrodes is reduced, thus reducing the dynamic resistance. If the liquid nugget is too large, the solid metal around it cannot hold it by welding force, causing the liquid to spill and accruing expulsion. On the other hand, the initial drop in electrode displacement is due to the application of force to the sheets. Then, with increasing temperature and thermal expansion, the distance between the two electrodes increases and decreases after reaching its maximum value and after the formation of liquid nuggets. An expulsion can also speed up the decline [4]. According to the behavior of these two signals and especially the dynamic resistance during welding, increasing the nugget radius and decreasing it after reaching the maximum value is explained.
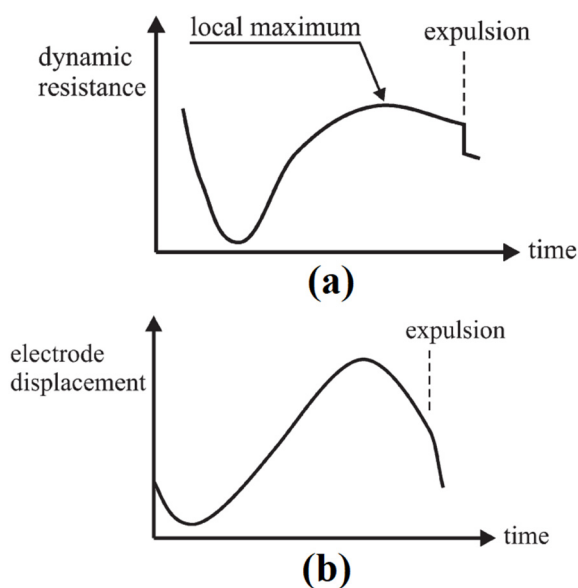

Fig. 10. Theoretical description of the signals, (a) Dynamic resistance; (b) Electrode displacement [31].

The effect of welding force increasing on the nugget radius is the opposite of the effect of current intensity. The electrode force changes during the welding process. The change in the dynamic electrode force is due to thermal expansion and the production of the weld zone at high temperature, so the dynamic electrode force is also important for the nugget size [18]. As the force increases, the contact between the two sheets increases and the resistance between them decreases, which reduces the generated heat and thus reduces the expansion of the nugget.

Electrode force, as an important welding parameter, could determine the contact state and dynamic resistance between sheets [21, 32]. Tang et al. [33] have studied the effect of welding force on dynamic and static resistance and have reported that with increasing force, the amount of these factors decreases and as a result, the generated heat also decreases.

Fig. 11 shows the interaction effect of welding parameters on the nugget radius. As mentioned earlier, only the interaction effect of welding time and welding force on the nugget radius is significant. As can be seen from the figure, when the welding time is short, the nugget radius increases with increasing welding force from 2 to 3 kN, but then with increasing force from 3 to 4 kN, the nugget radius decreases sharply. This interaction effect in longer welding times is such that by increasing the welding force from 2 to 4 kN, the nugget radius is strictly increasing. At short welding times due to the low softening of the steel, very small forces cannot increase the contact radius and therefore cannot reduce the dynamic resistance. Therefore, by increasing the force from 2 to 3 kN during at short welding time, temperature and nugget radius increase. On the other hand, in long welding times, due to the softening of the steel, any increase in force reduces the dynamic resistance and nugget radius [21]. ANOVA results for nugget thickness are shown in Table 2. The direct linear and quadratic effect of all parameters on the thickness is significant, but among the interaction effects, only the interaction effect of current intensity and welding time is significant. For nugget thickness, current intensity has the greatest effect (according to the F-value). Fig. 9(b) shows the direct effect of the parameters on the thickness. The effect of current intensity on the nugget thickness is similar to the effect of this parameter on the nugget radius. Increasing the current intensity increases the generated heat and as a result the nugget thickness increases, but as the current intensity approaches 10 kA due to the expulsion phenomenon the movement of the nugget towards the outer surfaces of the sheets stops. Stopping the increase or even decrease in the nugget thickness at high current intensities has also been reported in previous reports [19].

The effect of increasing the welding time on the nugget thickness, in contrast to its effect on the nugget radius, is always increasing. However, the

rate of increase in thickness is faster at shorter times than at longer times. Similar behavior has been reported in previous studies [19, 34]. In fact, increasing the time increases the generated heat and thickness. On the other hand, thermal expansion also, increases the nugget thickness. But in the long welding times, due to the melting of the nugget, the rate of increase in thickness decreases sharply. According to Fig. 9(b), the increase in force initially causes a slight increase in the thickness of the nugget, but then causes a sharp decrease. At low forces thermal expansion increases the thickness of the nugget but a high force not only increases the contact surface and thus reduces the resistance and generated heat, but also compresses the nugget and reduces its

thickness. The interaction effects of the parameters on the nugget thickness are shown in Fig. 12, of which only the interaction effect of current intensity and welding time is significant. At low current intensities, with increasing welding time, the thickness first decreases and then increases, but with increasing current intensity, the effect of increasing welding time is strictly upward. In fact, the rate of increase in nugget thickness is higher with increasing current intensity over long welding time. This shows that the effect of simultaneously increasing the time and current intensity causes a very large increase in the input heat by overcoming problems such as expulsions that reduce the thickness, increasing the thickness in each case.
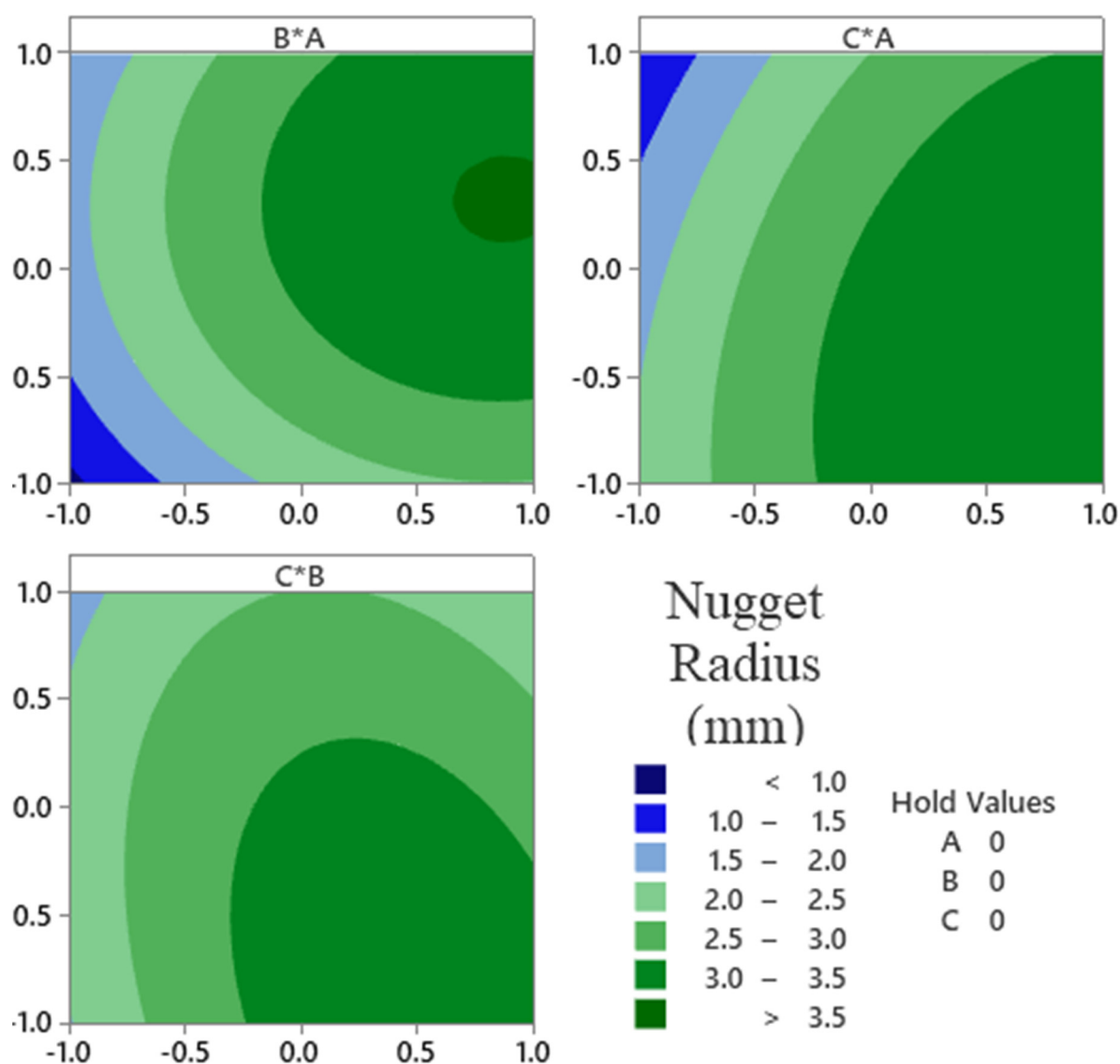

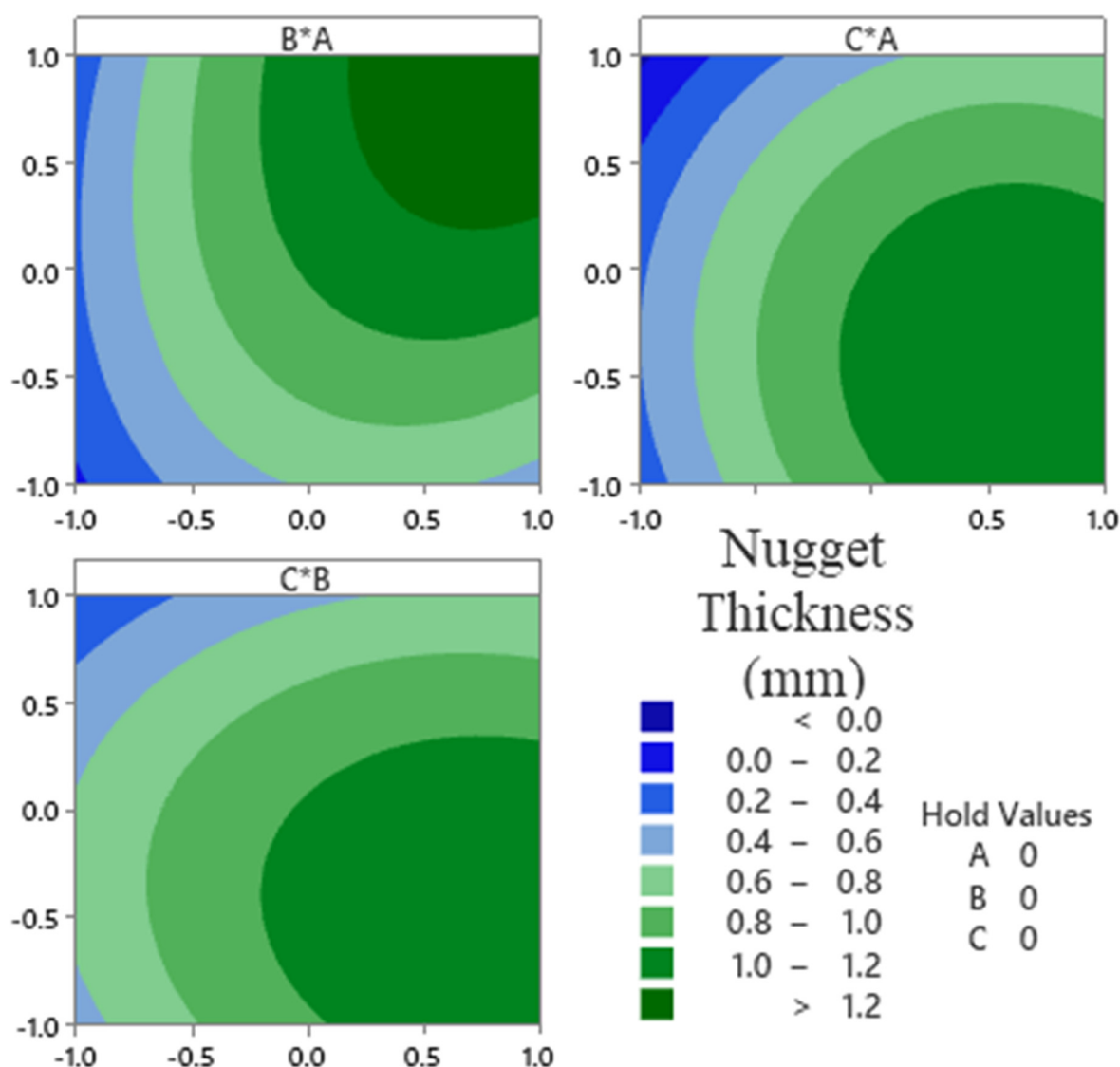**Fig. 11.** Contour plots showing the interaction effects of parameters on NZ radius.

Fig. 12. Contour plots showing the interaction effects of parameters on NZ thickness.

This can be seen in sample 4, where the current intensity and time are 10 kA and 30 cycles, respectively, which has the largest nugget thickness.

To obtain the nugget area, the nugget was assumed to be an ellipse with a large radius of the *nugget radius* and a small radius of the *nugget thickness*. In fact, the effect of parameters on the area is a combination of their effect on the radius and thickness of the nugget. According to Table 2, the direct and quadratic effect of all parameters on the area is significant and the only interaction effect that is significant is the effect of current intensity and time, although the interaction effect of time and force is also significant at level of 0.1 *p*-value. As can be seen from Table 2, the current intensity has the greatest effect on the area of the

nugget, which can be justified according to the role of this parameter in heat production. What is noteworthy is that the interaction effect of current intensity and time parameters on the area is more pronounced than the effect of interaction effects on other responses. Fig. 9(c) shows the direct linear effect of the parameters and Fig. 13 shows their interaction effects on nugget area.

According to Table 2, the direct linear and quadratic effects of all parameters on the HAZ radius are significant. Fig. 9(d) shows the direct effect of the parameters on the size of the HAZ radius. As can be seen, increasing the current intensity and welding time both increase the radius, but after reaching a maximum value, they reduce it. This trend is also seen in the effect of the welding force, with the difference that the

radius starts to decrease at small values of force. The effect of parameters on the HAZ radius is very similar to their effect on the nugget radius. The only significant difference in the low forces is that the increase in force, although the radius of the nugget remains constant, increases the radius of the HAZ.

Fig. 14 shows the interaction effect of the parameters on the HAZ radius. The interaction effect of current intensity and welding time as well as the interaction effect of time and force are significant. In short times, increasing the force causes the radius to increase first and then decreases, but in long times, increasing the force causes the radius to decrease continuously. It seems that long times and high forces cause the sheets to separate at longer distances and stop the progress of the HAZ. In fact, increasing the contact area near the tool (due to the compressive force of the electrodes) causes the sheets to separate at longer distances, which in turn prevents heat from spreading.
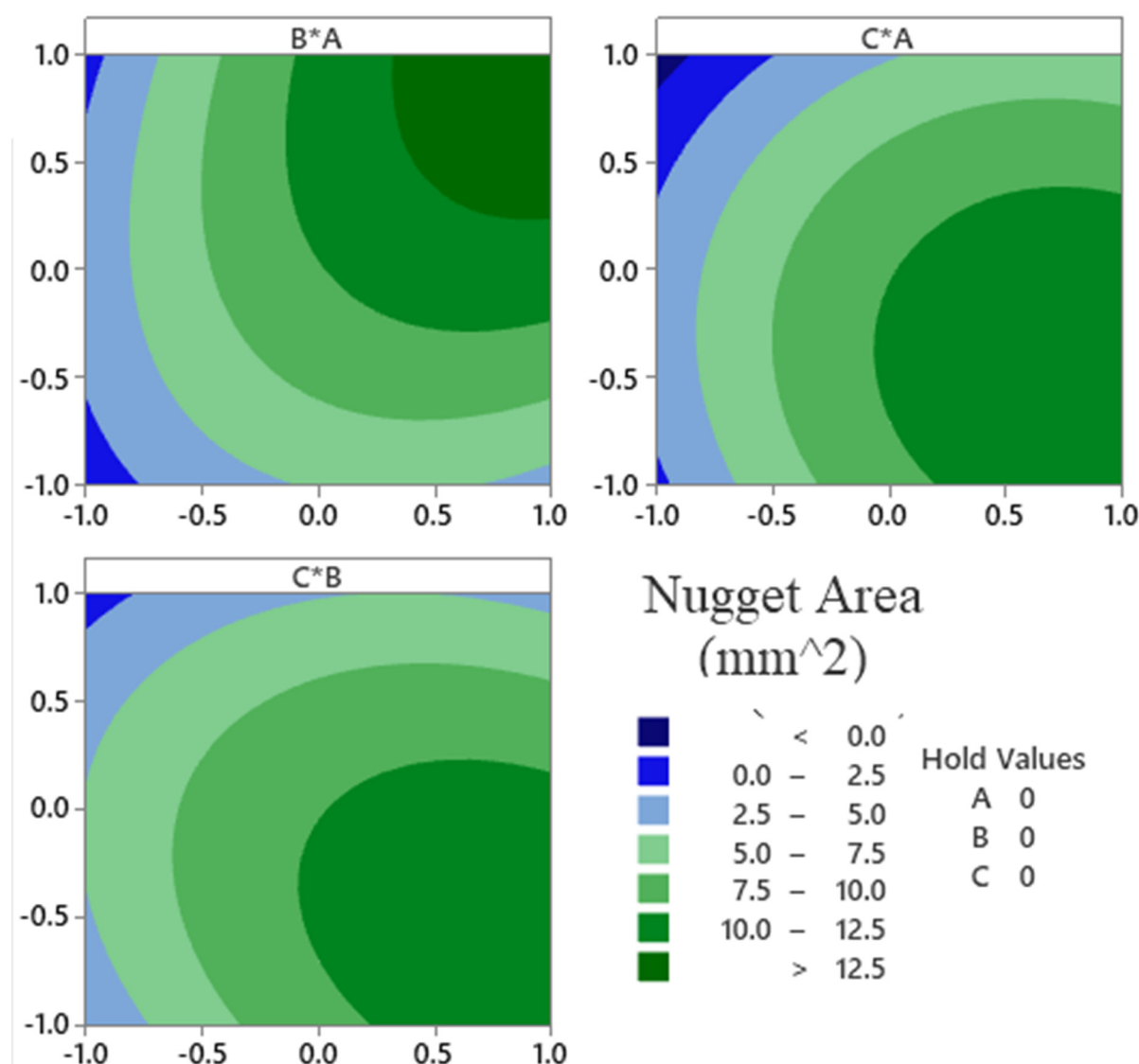

Fig. 13. Contour plots showing the interaction effects of parameters on NZ area.

4. CONCLUSIONS

- The effect of RSW parameters on the size of welding zones in TRIP steel joints, was investigated by DOE using the RSM and applying FE simulation. The input parameters were current intensity (A), welding time (B) and welding force (C). To validate the finite element model, two TRIP steel sheets were experimentally welded and the temperature

measured during the process was compared with the finite element results and a very good agreement was obtained.

- Examination of the microstructure of the weld zone in the experimental sample showed that two subdivided zone formed during welding: NZ and HAZ. Based on the critical temperatures, the NZ and HAZ were determined in all finite element models, and the Nugget radius, Nugget thickness, Nugget area, and HAZ radius were calculated. Using ANOVA, the direct, quadratic and interaction effect of parameters on the responses were evaluated and a mathematical model was extracted for each response.

- The direct linear effect of all parameters on all responses were significant. But among the interaction effects, the effect of B×C on the nugget radius, the effect of A×B on the nugget thickness, the effect of A×B on the nugget area and the effects of A×B and B×C on the HAZ radius were significant.

- Increasing the current intensity increased all the responses, but when the its value approached 10 kA, the responses decreased, which in most cases is related to the occurrence of expulsion and to prevent the spread of heat.

- Increasing the welding time continuously increased the nugget thickness, but in other responses it first increased and then decreased the size of the response.

- The effect of increasing the welding force was completely different from the effect of the other two parameters. Increasing the force, although initially increased the responses slightly (except for the nugget radius, which remained constant at first), but very soon due to increasing the contact surface of the sheets and reducing the electrical resistance reduced the heat generation and thus reduced the size of the zones.

COMPLIANCE WITH ETHICAL STANDARDS

REFERENCES

[1]. Soleimani M., Kalhor A., Mirzadeh H., "Transformation-induced plasticity (TRIP) in advanced steels: a review."Mater. Sci. Eng., A, 2020. 140023.

[2]. Ebrahimpour A., Mostafapour A., Nakhaei M. R., "Application of response surface methodology for weld strength prediction in FSSWed TRIP steel joints."Weld World, 2021. 65, 183-198.

[3]. Mostafapour A., Ebrahimpour A., Saeid T., "Finite element investigation on the effect of FSSW parameters on the size of welding subdivided zones in TRIP steels."Int. J. Adv. Manuf. Technol., 2017. 88, 277-289.

[4]. Zhou K., Yao P., "Overview of recent advances of process analysis and quality control in resistance spot welding."Mech Syst Signal Process, 2019. 124, 170-198.

[5]. Li Y., Lin Z., Shen Q., Lai X., "Numerical analysis of transport phenomena in resistance spot welding process."J Manuf Sci Eng, 2011. 133, 1-8.

[6]. Wan Z., Wang H.-P., Wang M., Carlson B. E., Sigler D. R., "Numerical simulation of resistance spot welding of Al to zinc-coated steel with improved representation of contact interactions."Int. J. Heat Mass Transfer, 2016. 101, 749-763.

[7]. Dickinson D., Franklin J., Stanya A., "Characterization of spot welding behavior by dynamic electrical parameter monitoring."Weld. J., 1980. 59, 170-176.

[8]. Kaars J., Mayr P., Koppe K., "Generalized dynamic transition resistance in spot welding of aluminized 22MnB5."Mater. Des., 2016. 106, 139-145.

[9]. Kang J., Shi L., Shalchi-Amirkhiz B., Sigler D., Haselhuhn A., Carlson B., "Microstructure and shear strength of novel aluminum to steel resistance spot welds."Weld. J., 2020. 99, 67-74.

[10]. Elitas M., Demir B., "The effects of the welding parameters on tensile properties of RSW junctions of DP1000 sheet steel."Eng. Technol. Appl. Sci. Res, 2018. 8, 3116-3120.

[11]. Raut M., Achwal V., "Optimization of spot welding process parameters for maximum tensile strength."Int. J. Mech. Eng. Robot. Res., 2014. 3, 506-517.

[12]. Thakur A., Rao T., Mukhedkar M., Nandedkar V., "Application of Taguchi method for resistance spot welding of galvanized steel."ARPN J. Eng. Appl. Sci. . 2010. 5, 22-26.

[13]. Akkaş N., "Welding Time Effect on Tensile–Shear Loading in Resistance Spot Welding of SPA-H Weathering Steel Sheets Used in Railway Vehicles"."Acta Phys. Pol., A, 2017. 131, 52-54.

[14]. Ashiri R., Mostaan H., Park Y.-D., "A phenomenological study of weld discontinuities and defects in resistance spot welding of advanced high strength TRIP steel."Metall. Mater. Trans. A, 2018. 49, 6161-6172.

[15]. Russo Spena P., De Maddis M., D'Antonio G., Lombardi F., "Weldability and monitoring of resistance spot welding of Q&P and TRIP steels."Met. Mater. Int., 2016. 6, 270-285.

[16]. Ashiri R., Marashi S., Park Y., "Weld processing and mechanical responses of 1-GPa TRIP steel resistance spot welds."Weld. J., 2018. 97, 157-169.

[17]. Akkaş N., Ferik E., İlhan E., Aslanlar S., "The effect of welding current on nugget sizes in resistance spot welding of spa-c steel sheets used in railway vehicles."Acta Phys. Pol., A, 2016. 130, 142-144.

[18]. Wen J., De Jia H., Wang C. S., "Quality Estimation System for Resistance Spot Welding of Stainless Steel." ISIJ International, 2019. 59, 2073-2076.

[19]. Eisazadeh H., Hamedi M., Halvaee A., "New parametric study of nugget size in resistance spot welding process using finite element method."Mater. Des., 2010. 31, 149-157.

[20]. Eshraghi M., Tschopp M. A., Zaeem M. A., Felicelli S. D., "Effect of resistance spot welding parameters on weld pool properties in a DP600 dual-phase steel: a parametric study using thermomechanically-coupled finite element analysis."Mater. Des., 2014. 56, 387-397.

[21]. Zhang Y., Shen J., Lai X., "Influence of electrode force on weld expulsion in resistance spot welding of dual phase steel with initial gap using simulation and experimental method."ISIJ international,

2012. 52, 493-498.

[22]. Mostafapour A., Ebrahimpour A., "The Effect of Two-stage Heat Treatment Temperatures on Initial and FSSWed Properties of TRIP Steels."Iron steel soc. iran., 2017. 14, 1-9.

[23]. Mostafapour A., Ebrahimpour A., Saeid T., "Numerical and experimental study on the effects of welding environment and input heat on properties of FSSWed TRIP steel."Int. J. Adv. Manuf. Technol., 2017. 90, 1131-1143.

[24]. Tumuluru M., "Resistance spot welding techniques for advanced high-strength steels (AHSS)."Weld. Join. AHSS., 2015. 1, 55-70.

[25]. Khan M., Kuntz M., Su P., Gerlich A., North T., Zhou Y., "Resistance and friction stir spot welding of DP600: a comparative study."Sci. Technol. Weld. Joining, 2007. 12, 175-182.

[26]. Jafari M., Arayee A., Senkara J., "A review of finite element analysis (FEA) of resistance spot welding (RSW)."Weld. Tech. Rev., 2016. 88, 46-52.

[27]. Ebrahimpour A., Mostafapour A., Samadian K., "Finite element and experimental investigation on the effects of temperature, strain and strain rate on microstructure and mechanical properties of FSSWed TRIP steel joints."Mater. Res. Express, 2019. 6, 016559.

[28]. Valaee-Tale M., Sheikhi M., Mazaheri Y., Ghaini F. M., Usefifar G. R., "Criterion for predicting expulsion in resistance spot welding of steel sheets."J. Mater. Process. Technol., 2020. 275, 116329.

[29]. Williams N., Parker J., "Review of resistance spot welding of steel sheets Part 1 Modelling and control of weld nugget formation."Int. Mater. Rev., 2004. 49, 45-75.

[30]. Wan X., Wang Y., Zhang P., "Modelling the effect of welding current on resistance spot welding of DP600 steel."J. Mater. Process. Technol., 2014. 214, 2723-2729.

[31]. Podržaj P., Polajnar I., Diaci J., Kariž Z., "Overview of resistance spot welding control."Sci. Technol. Weld. Joining, 2008. 13, 215-224.

[32]. Shome M., Chatterjee S., "Effect of material properties on contact resistance

and nugget size during spot welding of low carbon coated steels."ISIJ international, 2009. 49, 1384-1391.

[33]. Tang H., Hou W., Hu S., "Forging force in resistance spot welding."Proceedings of the Institution of Mechanical Engineers, Part B: Journal of Engineering Manufacture, 2002. 216, 957-968.

[34]. Gould J., "An examination of nugget development during spot welding, using both experimental and analytical techniques."Weld. J., 1987. 66, 1s-10s.

18